PHILOSOPHICAL TRANSACTIONS OF THE ROYAL SOCIETY A MATHEMATICAL, PHYSICAL & ENGINEERING SCIENCES

The Compositions of Barrier-Type Anodic Films Formed on Aluminium in Molybdate and Tungstate Electrolytes

G. E. Thompson, P. Skeldon, K. Shimizu and G. C. Wood

Phil. Trans. R. Soc. Lond. A 1995 **350**, 143-168
doi: 10.1098/rsta.1995.0005

The compositions of barrier-type anodic films formed on aluminium in molybdate and tungstate electrolytes

By G. E. Thompson, P. Skeldon, K. Shimizu and G. C. Wood

Corrosion and Protection Centre, UMIST, P.O. Box 88, Manchester M60 1QD, U.K.

During the formation of barrier-type anodic films on aluminium, low concentrations of electrolyte species, derived from electrolyte anions, are incorporated into the film. The incorporation process and the subsequent behaviour of the electrolyte species are of great relevance to understanding the mechanism of film formation and related phenomena, such as dielectric breakdown. This paper considers the incorporation of electrolyte species from molybdate and tungstate electrolytes. A capacitor model of the film is proposed to explain the resultant compositions of the films, which are dependent upon the concentration of adsorbed anions at the film surface. Using Rutherford backscattering spectroscopy, it is shown that molybdenum and tungsten species are incorporated into films at similar, constant rates, but their distributions in the films differ owing to their different mobilities. Both species migrate as cations by a cooperative transport mechanism involving also Al^{3+} and O^{2-}/OH^{-} ions. The compositions of the films depend upon the current density and the concentration, pH and temperature of the electrolyte although, for all conditions, only small amounts of electrolyte species are incorporated. The key role of the composition of the electrolyte at the film surface, which is significantly modified compared with the composition of the bulk electrolyte, is highlighted by preferential incorporation during film formation in the presence of both molybdate and tungstate ions.

1. Introduction

The kinetics of anodic film formation on the valve metals are commonly described by the high-field conduction equation,

$$J = A\exp(bE), \tag{1.1}$$

in which J is the ionic current density, E is the electric field strength and A and b are temperature-dependent constants. To satisfy this high-field conduction mechanism, the oxidation rate is determined by the migration of a charged 'defect' across a critical energy barrier that may be located in the film or at an interface. The equation has been extended empirically to include a quadratic term in the field (Young 1960; Dignam *et al.* 1965). This has been variously interpreted without affecting the model fundamentally (Dell'Oca & Young 1970).

Initially, ionic migration in anodic films was thought to be due to movements

Phil. Trans. R. Soc. Lond. A (1995) **350**, 143–168
Printed in Great Britain

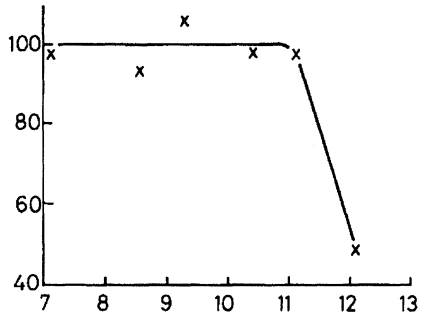

Figure 1. The effect of pH on the efficiency of film formation at 50 A m^{-2} in 10^{-2} M tungstate electrolytes at 293 K.

of simple defects, familiar from studies of diffusion in crystalline matter, such as Frenkel pairs (Young 1960). This view is satisfactory provided only either the anions or the cations in the film are mobile. Since in reality both anions and cations are usually mobile (Davies *et al.* 1965) and further, their transport numbers are relatively independent of the electric field (Pringle 1973), it is realized that a different form of defect is involved (Young & Smith 1979). Therefore, attention is now focused on so-called cooperative transport mechanisms, whereby a single activation event effectively controls migration of both anions and cations (Dignam 1972; Fromhold 1980; Mott 1987; Perriere *et al.* 1987). The proposed mechanisms typically involve structural changes in the film, possibly associated with loss of rigidity or liquid-like behaviour, that facilitate both anionic and cationic migration. However, the precise mechanisms of ionic transport are still unresolved. Therefore studies of anodic film formation are of continuing fundamental interest, particularly for those films which also have important practical applications, such as on aluminium.

Barrier-type anodic films, formed at ambient temperature on aluminium, are amorphous and are composed mainly of Al_2O_3. The transport numbers of Al^{3+} ions out and O^{2-}/OH^- ions in are relatively similar (Davies *et al.* 1965). There are no short-circuit paths through the film for ionic transport, which is uniform and by a short-range mechanism (Amsel & Samuel 1962). When the applied current results solely in film formation, i.e. at 100% Faradaic efficiency, new film material develops at both the metal–film and film–electrolyte interfaces. In common with other valve metals, small amounts of electrolyte species are incorporated into the film at the film–electrolyte interface during anodizing, e.g. boron species from borate electrolyte (Konno *et al.* 1980). Although derived from electrolyte anions, the incorporated electrolyte species can be immobile, migrate inwards or migrate outwards (Skeldon *et al.* 1985), and may have different valence states from those in the electrolyte (Chung *et al.* 1991). Incorporation can therefore involve chemical and electrochemical transformations at the film surface, or within the film, to produce new species. Studies of these transformations, and the subsequent behaviour of species in the film, assist the understanding of the mechanism of film formation and the nature of anodic alumina. The incorporation of electrolyte species may be important also in related phenomena, such as dielectric breakdown (Montero *et al.* 1985) and photo-current production (Di Quarto *et al.* 1992).

In the present experiments, the incorporation of molybdenum and tungsten species is investigated systematically for a range of anodizing conditions using aqueous molybdate and tungstate electrolytes. Molybdenum and tungsten species are examples of cationic electrolyte species that move outwards in the film during anodizing; the former species migrates more rapidly than the latter (Skeldon *et al.* 1985). These electrolytes were chosen because (i) films can be formed at similar nm V^{-1} ratios and at 100% efficiency, (ii) molybdenum and tungsten are incorporated at constant rates into the outer band of film material, in which they are distributed uniformly (Skeldon *et al.* 1989), and (iii) molybdenum and tungsten can be detected readily, quantitatively by Rutherford backscattering spectroscopy (RBS) and qualitatively, but with high spatial resolution, by transmission electron microscopy (Shimizu *et al.* 1981).

2. Experimental

(*a*) *Specimen preparation*

Superpure aluminium foils (0.004 w/o Cu, 0.003 w/o Fe, 0.002 w/o Si), of dimensions 20 mm × 10 mm, were electropolished at 15 V for 120 s in 80% ethanol/20% perchloric acid at 273–278 K. They were then rinsed in ethanol, doubly distilled water and AR grade acetone, and dried in a cool air stream. Foils were anodized at constant current density in stirred, aqueous electrolytes, prepared with doubly distilled water and AR grade sodium molybdate ($Na_2MoO_4.2H_2O$) or sodium tungstate ($Na_2WO_4.2H_2O$). The pH values of 10^{-1} M solutions were 7.5 and 9.3 respectively. When necessary, the pH values of the electrolytes were adjusted by addition of sodium hydroxide.

Foils were anodized in molybdate electrolyte to 175 V and in tungstate electrolytes to voltages up to the dielectric breakdown voltages. The breakdown voltages were, approximately, 285, 435, 530, 670 and 860 V for electrolyte concentrations of 10^{-1}, 10^{-2}, 10^{-3}, 10^{-4} and 10^{-5} M, and were not significantly influenced by the pH of the electrolyte. Anodizing was stopped when sparks were first seen, to avoid any influence of prolonged breakdown on the resultant film compositions. Other experiments, described later, were also carried out using mixtures of molybdate and tungstate electrolytes. After anodizing, foils were immediately removed from the electrolyte and rinsed in doubly distilled water and AR grade acetone. For the most accurate analyses by RBS, self-supporting films were prepared to eliminate background scattering from the substrate (Shimizu *et al.* 1982); otherwise films were analysed in the as-anodized condition.

The efficiency of film formation was determined by comparing the slopes of the voltage–time curves with those predicted using published data for the kinetics of anodizing at *ca.* 100% efficiency in borate electrolyte (Harkness & Young 1966). The film density was assumed to be 3100 kg m^{-3}. To an accuracy of ±5%, films formed at 100% efficiency, except for anodizing in tungstate electrolytes of pH > 11, as shown in figure 1.

(*b*) *Compositions of films by Rutherford backscattering spectroscopy*

Films were analysed using 2.0 MeV alpha particles supplied by the 7 MeV Van de Graaff accelerator that was located at the University of Manchester. The beam current and diameter were about 3 nA and 0.5 mm respectively. The beam was

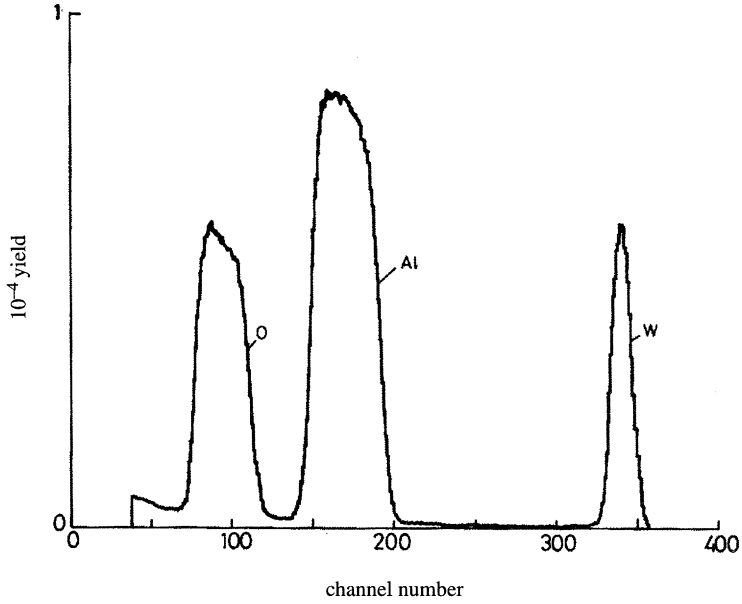

Figure 2. Energy spectrum of 2.0 MeV alpha particles elastically scattered from a self-supporting film formed at 50 A m^{-2} to 250 V in 10^{-1} M tungstate electrolyte at 293 K.

usually at normal incidence on the film surface. Elastically scattered alpha particles were detected at 165° by a silicon surface barrier detector. A pre-amplifier, amplifier and analogue-to-digital converter processed signals for accumulation of the energy spectra by a PDP 11 computer. The use of RBS for the analysis of anodic films is described in Appendix A.

(*c*) *Transmission electron microscopy*

Film sections attached to the aluminium substrate were prepared on an LKB III ultramicrotome by the usual procedure (Furneaux *et al.* 1978). They were examined in a Philips 301 transmission electron microscope (TEM), operating at 100 kV.

3. Results

(*a*) *Compositions of films formed in* 10^{-1} M *molybdate and tungstate electrolytes at* 293 K

The compositions of self-supporting films formed at 50 A m^{-2} were determined by RBS. For these films, it is known that molybdenum and tungsten are contained in the outer 0.2 and 0.3 of the film thickness respectively (Shimizu *et al.* 1981; Skeldon *et al.* 1985). An energy spectrum of elastically scattered alpha particles from a film containing tungsten is shown in figure 2.

The figure shows three separated peaks due to scattering from oxygen, aluminium and tungsten nuclei in the film. The alpha particle energy increases with the atomic weight of the scattering nuclei. Alpha particles scattered from nuclei in the film surface have the highest energy. Those scattered from nuclei in internal layers have lower energies because of the losses in penetrating and emerging from

the film. For thin films, the energy losses are linearly dependent upon the layer depth and hence, distributions of species can be determined (see Appendix A). Because tungsten is contained in the outer 0.3 of the film thickness, the width of the tungsten peak is less than those for aluminium and oxygen, which are distributed throughout the film. Tungsten gives a strong signal, although the concentration in the film is low, because the cross-section for elastic scattering is proportional to Z^2, where Z is the atomic number of the scattering nucleus.

The compositions that were determined for films formed to 175 and 250 V in molybdate and tungstate electrolytes respectively can be expressed as:

$$Al_2O_3 \,.\, 0.013 \pm 0.001 \quad (MoO_{4\pm2}),$$
$$Al_2O_3 \,.\, 0.015 \pm 0.001 \quad (WO_{3\pm1}).$$

These are the averages of analyses of two films of each type. The expressions are derived from the measured atomic ratios of the constituents of the film, assuming that aluminium is present as Al_2O_3. The average atomic ratios of Mo/Al and W/Al are similar, corresponding to about 7×10^{-3}. (This method of presenting film compositions is usually followed throughout the study, and such compositions are referred to as average concentrations of molybdenum or tungsten. However, occasionally reference is made to point concentrations, which are the atomic ratios of either Mo/Al or W/Al within the region of film containing the electrolyte species.) Since the molybdenum and tungsten are contained in layers of differing relative thickness, the point concentrations of molybdenum and tungsten differ significantly; these are 3.3×10^{-2} and 2.5×10^{-2} respectively. Therefore, the point concentration of molybdenum is about 30% higher than that of tungsten. This is due to the higher mobility of molybdenum in the film compared with that of tungsten, which is discussed later.

Theoretical profiles for the peaks due to elastic scattering of alpha particles from aluminium and oxygen are compared with the experimental profiles, for a film formed in tungstate electrolyte, in figure 3. The calculations of the theoretical shapes, by computer program, included the effects of detector resolution, straggling, and the dependence upon energy of both the elastic scattering cross-section and stopping power. The calculations were made for a pure Al_2O_3 film, with a density of 3100 kg m^{-2} and a thickness of 300 nm. The thickness corresponds to a formation ratio of 1.2 nm V^{-1}, that is typical for barrier-type films on aluminium. The experimental and theoretical profiles are similar for the oxygen peak but for the aluminium peak, the experimental data are about 3% lower in the region corresponding to scattering from the outer 0.3 of the film thickness. This difference is due to the presence of tungsten in the outer part of the film.

(*b*) *Effects of anodizing conditions on film compositions*

In the following, the average concentrations of tungsten are reported for films attached to their substrates. The films were formed in tungstate electrolytes over a range of anodizing conditions in which the current density and the concentration, pH and temperature of the electrolyte were varied. The error bars on figures indicate the 95% confidence limits. The effect of temperature on the film composition is shown in figure 4. The films were formed to 200 V at 50 A m^{-2} in 10^{-1} M tungstate electrolyte at 273–323 K. The concentration of tungsten in-

PHILOSOPHICAL TRANSACTIONS OF THE ROYAL SOCIETY A MATHEMATICAL, PHYSICAL & ENGINEERING SCIENCES

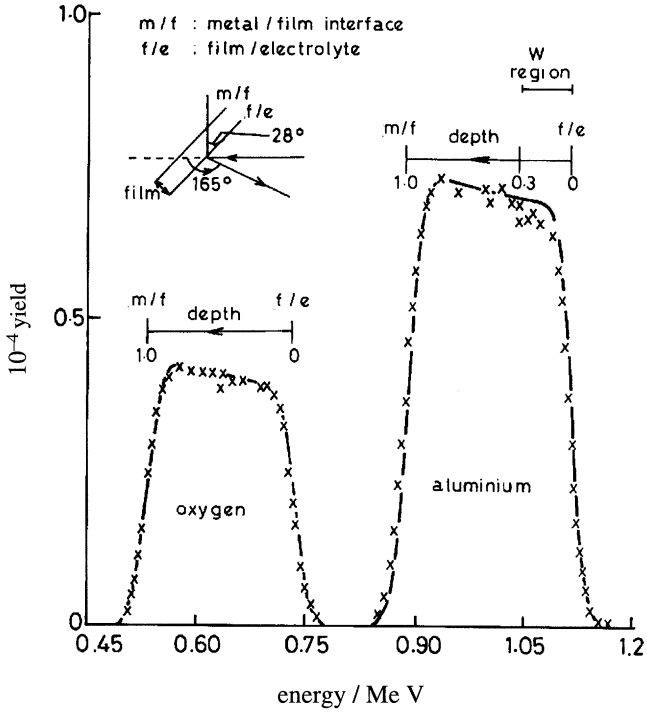

Figure 3. Comparison of experimental and theoretical shapes of the peaks, due to elastic scattering of 2.0 MeV alpha particles from aluminium and oxygen, in a film formed at 50 A m^{-2} to 250 V in 10^{-1} M tungstate electrolyte at 293 K.

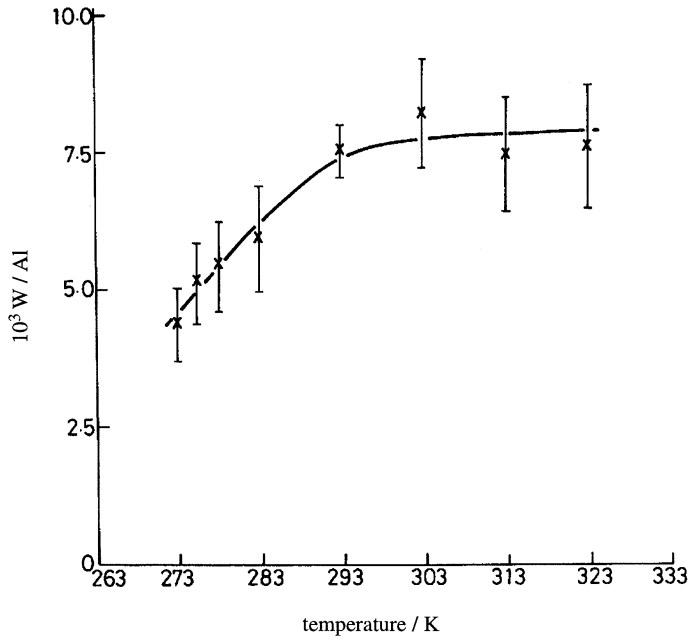

Figure 4. The effect of electrolyte temperature on the average atomic ratio of W/Al in films formed at 50 A m^{-2} to 200 V in 10^{-1} M tungstate electrolyte.

PHILOSOPHICAL TRANSACTIONS OF THE ROYAL SOCIETY A MATHEMATICAL, PHYSICAL & ENGINEERING SCIENCES

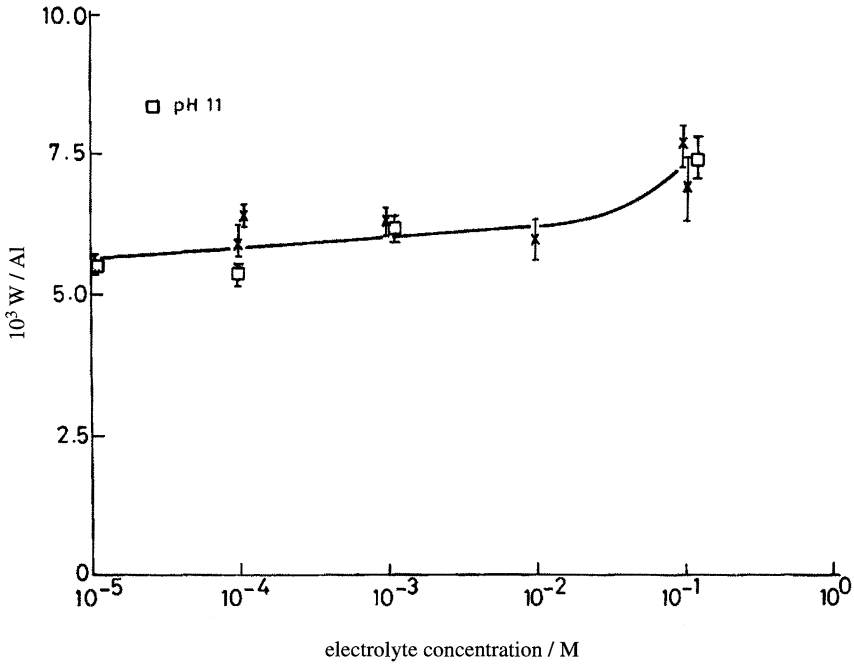

Figure 5. The effect of electrolyte concentration and pH on the average atomic ratio of W/Al in films formed at 50 A m^{-2} to the breakdown voltages in tungstate electrolyte at 293 K.

creases by about 50% between 273 and 293 K. Subsequently, the film composition is relatively independent of temperature.

The effect of the concentration of tungstate ions in the electrolyte on the film composition was examined over the range 10^{-4}–10^{-1} M, corresponding to pH values between 6.5 and 9.3, and also over the range 10^{-5}–10^{-1} M with the pH adjusted to 11. The films were formed at 293 K to the breakdown voltages using a current density of 50 A m^{-2}. The results, shown in figure 5, reveal that the average concentration of tungsten in the film increases by about 35% between electrolyte concentrations of 10^{-5}–10^{-1} M. The greatest change in film composition occurs between 10^{-2} and 10^{-1} M. Raising the pH to 11 has no significant effect on the film composition.

Further studies of the effect of pH on the film composition, under the same general anodizing conditions, were carried out using 10^{-2} M tungstate electrolytes of pH in the range 8.6–12.1. The results, shown in figure 6, and the previous results of figure 5, indicate that the effect of pH is negligible between pH values of 8.6–11. Above pH 11, when the efficiency of film formation is less than 100%, the average concentration of tungsten decreases rapidly to a relatively low level at pH 12.1. The film formed at pH 12.1 was about 15% thicker than others, as determined by RBS (see Appendix A), probably due to a porous/precipitated surface layer. At this pH, as will be explained, there is no mechanism for incorporation of tungsten and the traces detected are residual electrolyte contamination.

The effect of current density on the film composition was studied between 1 and 1000 A m^{-2}. The films were formed to 200 V at 293 K in 10^{-1} M tungstate electrolyte. The results, shown in figure 7, reveal that the average concentration

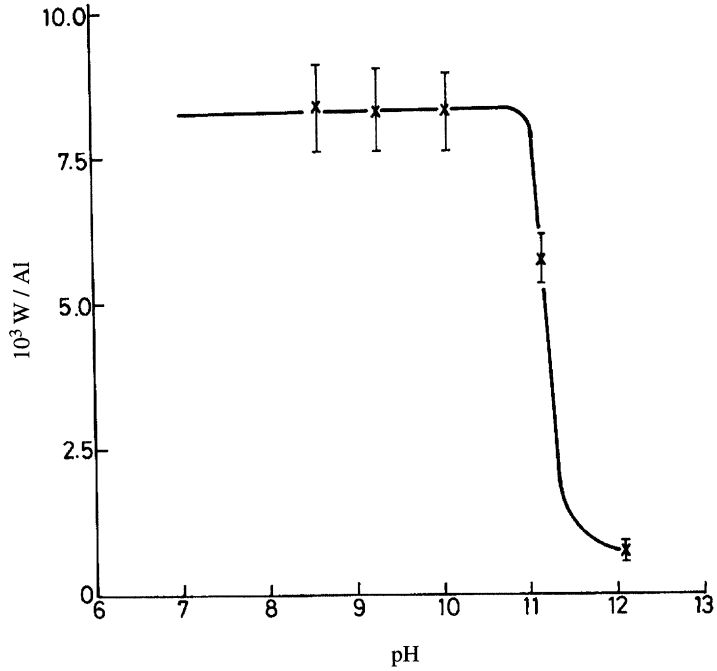

Figure 6. The effect of electrolyte pH on the average atomic ratio of W/Al in films formed at 50 A m^{-2} to the breakdown voltage in 10^{-2} M tungstate electrolyte at 293 K.

Table 1. *Average concentrations and distributions of tungsten in films formed to* 200 V *in* 10^{-1} M *tungstate electrolyte*

temp./K	current density/(A m^{-2})	composition of film, W:Al/10^{-3}	composition of inner film, W:Al/10^{-5}	distribution
323	50	8.2 ± 0.3	< 1.6	0.29 ± 0.04
273	50	5.5 ± 0.4	< 2.2	0.29 ± 0.04
293	20	7.7 ± 0.4	< 3.1	0.31 ± 0.04
293	1000	9.5 ± 0.8	< 3.8	0.30 ± 0.04
				mean= 0.30 ± 0.04

of tungsten in the film increases by about 15% between 20 and 1000 A m^{-2}. Below 10 A m^{-2}, there is a rapid increase in the amount of tungsten. As discussed later, the rapid rise in tungsten concentration is probably due to precipitation of tungsten oxide on the film surface.

(*c*) *Distribution of tungsten in films*

In this section the distributions of tungsten are presented for the films considered in the previous section, but excluding those films formed either at pH > 11 or at a current density of less than 10 A m^{-2}. The distributions in these latter films

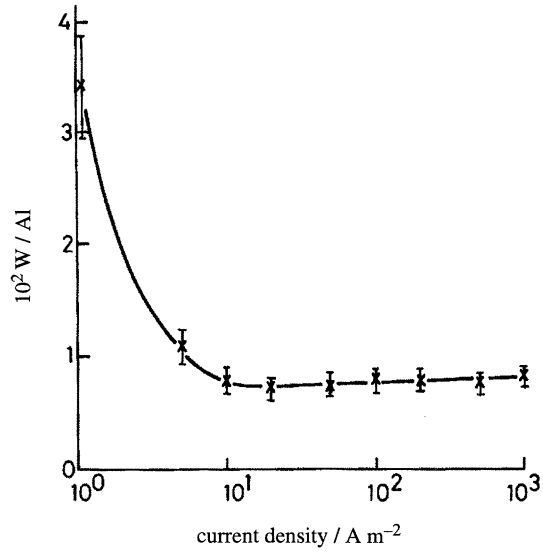

Figure 7. The effect of current density on the average atomic ratio of W/Al in films formed to 200 V in 10^{-1} M tungstate electrolyte at 293 K.

which may have been porous or contained surface precipitates are not of major interest here. The fraction of the film thickness containing tungsten was determined from the relative widths of the alpha particle yields due to aluminium and tungsten nuclei in the film (see Appendix A). For films formed to greater than 200 V, the distributions were derived from data used for analyses of compositions. For others, additional measurements were needed using an oblique angle of incidence of the alpha particle beam on the film surface in order to improve the depth resolution. Of particular interest are the results presented in table 1 for films formed at the extremes of current density and temperature, since these parameters are expected to have the greatest effect on ionic transport by a field-assisted diffusion mechanism. All error bars in the table represent the 95% confidence limits. An example of an energy spectrum of alpha particles for one of these specimens is shown in figure 8. The energy spectrum is interpreted similarly to that of the self-supporting film, but now a background is present from the substrate upon which the yield from oxygen in the film is superimposed. Importantly, from table 1, there are no significant differences between the distributions of tungsten in the various films. The mean value of 0.30 for the relative thickness of the layer of film containing tungsten, i.e. the thickness of the layer divided by the total film thickness, is the same as found in previous work for film formation at 50 A m^{-2} and at 293 K. Further, all other films examined, i.e. those formed over the ranges of electrolyte concentration and pH, contained similar distributions. Therefore, it can be concluded that the current density, and the temperature, concentration and pH of the electrolyte, have negligible effect on the distributions of tungsten in films which are formed at 100% efficiency. Table 1 also gives average film compositions that were determined from analyses of the composition of the outer band of film material containing tungsten (see Appendix A). These analyses exclude any possible influence of traces of adsorbed tungsten or other surface contamination. They confirm the increases in the average concentration of tungsten in

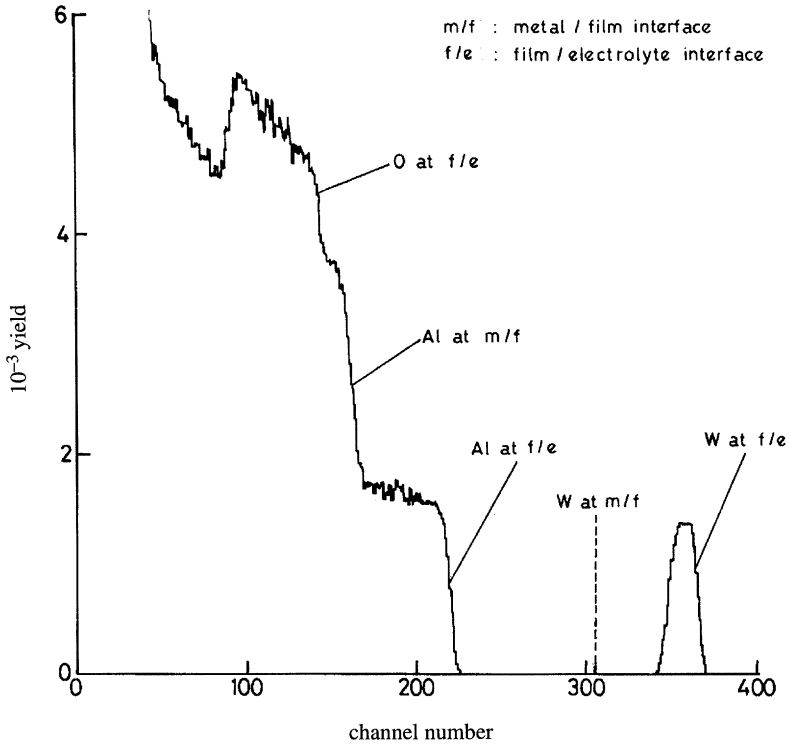

Figure 8. Energy spectrum of 2.0 MeV alpha particles elastically scattered from a specimen anodized at 50 A m^{-2} to 200 V in 10^{-1} M tungstate electrolyte at 323 K.

the films with increase of either current density or temperature that were found previously. Further, the table gives the upper limits for the average concentrations of tungsten in the inner 0.5 of the film thicknesses, which are determined by the background due to pile-up. The point concentration of tungsten in the inner half of the film is less than 0.2% of that in the outer 0.3 of the film thickness. In the depth region between relative thicknesses of 0.3–0.5, the detector resolution precluded giving a realistic upper limit on the tungsten concentration under the conditions of analysis. However, the sharpness of the boundary of the tungsten-containing region of film, observed by TEM (Shimizu *et al.* 1981), indicates that this intermediate region can only contain very low concentrations of tungsten.

(*d*) *Effect on film composition of anodizing in electrolytes containing both molybdate and tungstate ions*

The experiments to examine the effect on film composition of the presence of both molybdate and tungstate ions in solution comprised three types in all of which films were formed to 200 V at 100% efficiency. Firstly, anodizing was carried out in an electrolyte containing molybdate and tungstate ions in equal concentrations of 5×10^{-2} M, using a current density of either 50 A m^{-2} or 200 A m^{-2}. The purpose of these experiments was to determine the effect of current density on the film composition. The results, given for samples 1 and 2 in table 2, in which the errors indicate one standard deviation, show that both molybdenum

Table 2. *Average concentration of molybdenum and tungsten in films formed to* 200 V *at* 293 K *in electrolytes containing both molybdate and tungstate ions*

	electrolyte composition/M		current density	film composition		
spec.	MoO_4^{2-}	WO_4^{2-}	A m^{-2}	Mo/Al	W/Al	Mo/W
1	5×10^{-2}	5×10^{-2}	50	$1.2 \pm 0.1 \times 10^{-3}$	$6.2 \pm 0.1 \times 10^{-3}$	0.19 ± 0.0
2	5×10^{-2}	5×10^{-2}	200	$5.2 \pm 0.2 \times 10^{-3}$	$1.6 \pm 0.3 \times 10^{-3}$	3.3 ± 0.6
3	5×10^{-4}	5×10^{-4}	200	$5.3 \pm 0.2 \times 10^{-3}$	$1.3 \pm 0.2 \times 10^{-3}$	4.1 ± 0.7
4[a]	5×10^{-6}	5×10^{-6}	200	$5.6 \pm 0.2 \times 10^{-3}$	$1.2 \pm 0.3 \times 10^{-3}$	4.7 ± 1.2
5	5×10^{-2}	5×10^{-3}	50	$6.9 \pm 0.4 \times 10^{-3}$	$< 3 \times 10^{-4}$	> 23
6	5×10^{-2}	5×10^{-4}	50	$6.8 \pm 0.5 \times 10^{-3}$	$< 3 \times 10^{-4}$	> 23
7	5×10^{-2}	5×10^{-5}	50	$7.5 \pm 0.4 \times 10^{-3}$	$< 3 \times 10^{-4}$	> 25

[a]pH 11.

and tungsten species are incorporated into the film. However, although equal concentrations of molybdate and tungstate ions are present in the bulk electrolyte, the average concentrations of molybdenum and tungsten in the films reveal preferential incorporation of one species. Importantly, the preferred species depends upon the current density. At the lower current density, the film contains about 5.3 times more tungsten than molybdenum but, at the higher current density, preferential incorporation is reversed and the film now contains about 3.3 times more molybdenum than tungsten.

A second group of experiments determined whether the preferred incorporation of molybdenum species at the high current density persisted during anodizing in more dilute electrolytes. Thus, films were formed at 200 A m^{-2} in electrolytes containing equal concentrations of molybdate and tungstate ions, but in more dilute solutions. Preferential incorporation of molybdenum species again occurred, to a similar or possibly slightly greater extent compared with the more concentrated mixture, as shown in table 2 by specimens 3 and 4.

Finally, experiments were carried out to determine whether preferential incorporation of tungsten species was still possible, during anodizing at the lower current density, if tungstate ions were the minority ions in the bulk electrolyte. The results, given in table 2 by specimens 5, 6 and 7, indicate that preferential incorporation of tungsten no longer occurs when the electrolyte composition is dominated by molybdate ions. For this last group of specimens, only small amounts of tungsten were detected that are due mainly to residual surface contamination rather than incorporated species. This was evident from the absence of any change in the peak width as the sample was angled to the beam. Hence, upper limits are given for the amounts of tungsten incorporated in these films. Significantly, from table 1, the combined total amount of molybdenum and tungsten in the film is the same as the amount of either molybdenum or tungsten in films formed in the respective individual electrolytes, i.e. an atomic ratio with respect to aluminium of about 7×10^{-3}. Thus, anodizing in the mixed electrolytes does not enhance the total concentration of the electrolyte species in the film. Therefore, although preferential incorporation of a particular species can occur

PHILOSOPHICAL TRANSACTIONS OF THE ROYAL SOCIETY A MATHEMATICAL, PHYSICAL & ENGINEERING SCIENCES

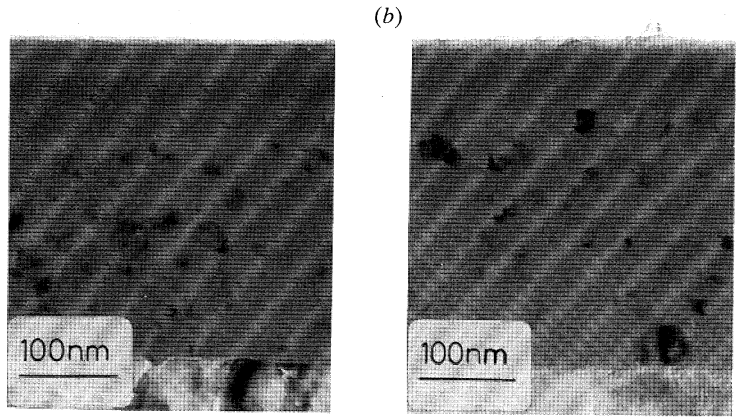

Figure 9. Transmission electron micrographs of an ultramicrotomed section of a film formed at 50 A m^{-2} to 285 V in an electrolyte containing 5×10^{-2} M of both molybdate and tungstate ions at 293 K and crystallized in the electron beam of the TEM. (*a*) Initial location of the boundary between crystallized and uncrystallized film material. (*b*) Subsequent location of the boundary on further exposure to the electron beam.

in mixed electrolytes, its concentration in the film never exceeds, and is usually less than, the concentration found for the individual electrolyte.

Notably, RBS indicated that molybdenum and tungsten are distributed in the films in the manner found after anodizing in the individual electrolytes, i.e. in the outer 0.20 ± 0.02 and 0.30 ± 0.02 of the film thickness. This was also confirmed by examination of a film in the TEM. Figure 9 shows ultramicrotomed sections of a film formed at 50 A m^{-2} to 285 V in a mixture containing 5×10^{-2} M of both molybdate and tungstate ions. The distributions of molybdenum and tungsten are revealed by crystallization of the relatively uncontaminated regions of film in the electron beam of the TEM. Two positions of the boundary between crystallized and uncrystallized film are found. The first occurs at a depth of 0.30 ± 0.02 of the film thickness (after correction for contraction of the thickness of the inner region due to crystallization) following initial exposure of the film to the electron beam. The second occurs at a depth of 0.20 ± 0.02, after further exposure of the film to the electron beam. These positions agree with the distributions of molybdenum and tungsten found by RBS. The sequential appearance of the boundaries can be related to the higher concentration of electrolyte species in the outermost band of film and/or greater stabilization of the amorphous structure by molybdenum species.

4. Discussion

(*a*) *Formation of barrier-type anodic films*

Barrier-type anodic films form on aluminium in aqueous electrolytes by migration of Al^{3+} and O^{2-}/OH^{-} ions across the film thickness, assisted by the electric field. The transport numbers of the ions are relatively similar and generally independent of the anodizing conditions normally used (Thompson *et al.* 1987). Nuclear tracer experiments have revealed that the order of aluminium and of oxygen isotopes in the films is conserved during anodizing, indicating that there are no short-circuit transport paths (Amsel & Samuel 1962). The films have flat and parallel metal–film and film–electrolyte interfaces, and are mainly composed

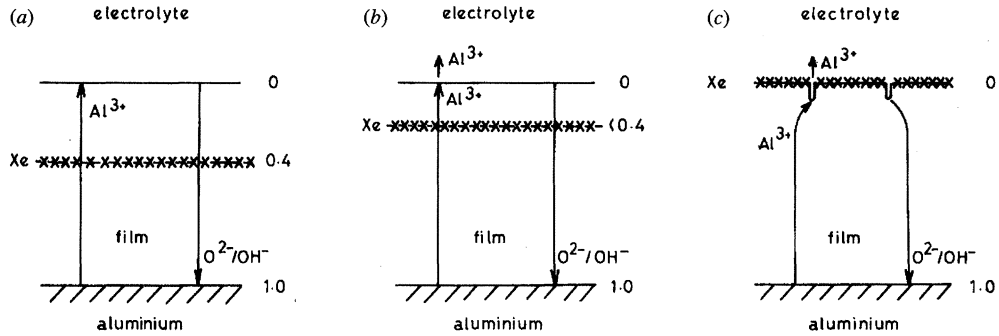

Figure 10. Schematic diagrams illustrating film formation. The arrows indicate the ionic fluxes. (*a*) At 100% efficiency; (*b*) at 60–100% efficiency; (*c*) at 60% efficiency.

of amorphous Al_2O_3. The sites of film formation have been identified by ion implanting a narrow band of xenon into a thin film which acts as an immobile reference plane during subsequent anodizing (Brown & Mackintosh 1973; Shimizu *et al.* 1991). New film material forms at both the metal–film and film–electrolyte interfaces. For anodizing at 100% efficiency, about 0.4 of the film thickness is developed at the latter interface (Brown & Mackintosh 1973). This proportion decreases at lower efficiency. At efficiencies of not greater than 60%, no film material forms at the film surface and a porous film, rather than a barrier-type film, develops (Thompson *et al.* 1987).

The appearances in the TEM of films formed to similar voltages at different efficiencies are shown schematically in figure 10. Figure 10*a* illustrates a barrier-type film formed at 100% efficiency; Al^{3+} and O^{2-}/OH^- ions migrate across the film thickness to form new film material at both the metal–film and film–electrolyte interfaces. The xenon layer is located in the film at a relative depth of 0.4, indicating the cation and anion transport numbers are approximately 0.4 and 0.6 respectively. Figure 10*b* illustrates a barrier-type film formed at an efficiency between 60–100%. The xenon layer is now located nearer to the film surface, since only part of the Al^{3+} ion flux results in film formation at the film–electrolyte interface. The remainder of the Al^{3+} ion flux is directly ejected into the electrolyte. Although the apparent transport numbers of Al^{3+} and O^{2-}/OH^- ions, deduced from the location of the xenon layer, are now changed from those for formation at 100% efficiency, the true transport numbers, determined by including the directly ejected Al^{3+} ions in the mass balance, are unaltered. Figure 10*c* illustrates a film formed at not greater than 60% efficiency. No film material is formed at the film–electrolyte interface, and pores develop at the film surface. The geometry of the pores locally enhances the electric field, which gives rise to simultaneous field-assisted dissolution of the film and direct ejection of Al^{3+} ions at the pore bases. Subsequently, the classical porous alumina film is developed containing regular pores. The above transformations of the film morphology have been discussed in full previously (Thompson *et al.* 1987).

(*b*) *Distribution and mobilities of electrolyte species*

Certain regions of barrier-type film usually contain electrolyte species. The electrolyte species originate from the electrolyte anions that are either directly

PHILOSOPHICAL TRANSACTIONS OF THE ROYAL SOCIETY A MATHEMATICAL, PHYSICAL & ENGINEERING SCIENCES

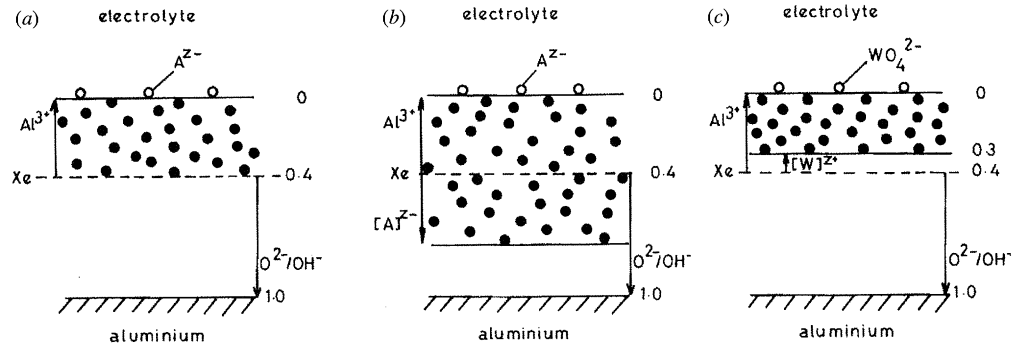

Figure 11. Schematic diagrams illustrating films formed at 100% efficiency. The arrows indicate the relative migration rates of electrolyte species and Al^{3+} and O^{2-}/OH^- ions. (*a*) Containing immobile electrolyte species. (*b*) Containing inwardly mobile electrolyte species $[A]^{Z-}$. (*c*) Containing outwardly mobile electrolyte species $[W]^{Z+}$.

incorporated into the film, or transformed into new forms during, or following, incorporation. Examples of species revealing inward migration, outward migration and immobility during anodizing are now well known (Skeldon *et al.* 1985). Commonly the electrolyte species are distributed uniformly in an outer band of film material that has a sharp boundary with the inner, uncontaminated region. Tungsten and molybdenum species are in this category. For formation at 100% efficiency, immobile electrolyte species are distributed in the outer 0.4 of the film thickness that is developed at the film–electrolyte interface. Mobile species are distributed over lesser or greater depths depending on whether they migrate as cations or anions. Exceptionally, irregular distributions are observed, in particular with antimony (Skeldon *et al.* 1993) and chromium species (Shimizu *et al.* 1990) that are contained in several bands of differing concentration.

Figure 11 shows schematically examples of films, formed at 100% efficiency, containing immobile, inwardly mobile and outwardly mobile electrolyte species. The mobility is determined by measuring the ionic movement with respect to the immobile xenon layer. Figure 11*a* illustrates a film containing immobile electrolyte species. The electrolyte species, derived from the adsorbed electrolyte anions, are incorporated at a constant rate into film material formed at the film–electrolyte interface. Since they are immobile in the film, they are distributed uniformly in the band of film material formed originally at the film–electrolyte interface. This band extends from the film surface to the xenon layer. Beneath the xenon layer, the film is composed of relatively pure anodic alumina. Figure 11*b* illustrates a film containing electrolyte species that migrate inwards during anodizing. The electrolyte anions are either directly incorporated into the film, or transformed to new kinds of anion. Since they migrate inwards, they move into the film material beneath the xenon layer. The electrolyte species migrate more slowly than O^{2-}/OH^- ions and a band of relatively pure anodic alumina is found adjacent to the metal–film interface. Figure 11*c* illustrates a film containing electrolyte species that migrate outwards during anodizing. The specific example of a film formed in tungstate electrolyte is used. The electrolyte anions are transformed to cation species during incorporation into the film. The electrolyte species migrate towards the film surface at a slower rate than Al^{3+} ions. The band

of relatively pure anodic alumina now extends from the metal–film interface to above the xenon layer. The region of this band above the xenon layer consists of film material that originally contained electrolyte species.

Although marker experiments are needed to determine accurately the mobility of tungsten over the range of anodizing conditions studied, as noted earlier, work in other electrolytes indicates that the transport numbers of Al^{3+} and O^{2-}/OH^{-} ions are not significantly affected by relatively large changes in anodizing conditions (Thompson *et al.* 1987) and typically about 0.4 of the film thickness forms at the film–electrolyte interface for anodizing at 100% efficiency. The present results show that molybdenum and tungsten are then contained in the outer 0.20 ± 0.02 and 0.30 ± 0.02 of the film thickness respectively and the distribution of tungsten is negligibly affected by temperature, electrolyte concentration, pH or current density. From the determined film compositions, the point concentrations of molybdenum and tungsten in their respective bands of film material are 3.5 and 2.3 at/o of the cations. These concentrations are below the percolation threshold for a random distribution of electrolyte species, at which current might flow along molybdenum-rich or tungsten-rich pathways. The presence of molybdenum and tungsten may reduce slightly the film resistivity, since MoO_3 and WO_3 are of lower resistivity than Al_2O_3 (Pringle 1980). Anodizing proceeds uniformly for this ordering of resistivities in the film unlike the opposite situation, with high resistivity material overlying a lower resistivity material, when current channelling occurs (Skeldon *et al.* 1990).

Although molybdenum and tungsten species are incorporated into films at approximately equal rates and in similar amounts, the local concentration of molybdenum is higher than that of tungsten in their respective films. This is because molybdenum moves outwards more rapidly than tungsten. The relative migration rates can be determined by consideration of the formation of the film illustrated in figure 11*c*, which shows schematically a film containing tungstate species. The outer 0.4 of the film thickness is developed by adding sequentially new layers of film material at the film–electrolyte interface. At the start of anodizing, the first layer formed at the film–electrolyte interface contains both Al^{3+} ions and incorporated tungsten species. The following layer contains Al^{3+} ions that have migrated from the initial layer and freshly incorporated electrolyte species. Subsequent layers form in the same manner, with the initial Al^{3+} ions remaining at the film surface since cation order is conserved. Tungsten species, however, migrate outwards more slowly than Al^{3+} ions, otherwise they also would remain at the film surface rather than being found within the alumina. The tungsten species are progressively left behind by the more mobile Al^{3+} ions at the film surface. The tungsten species introduced first are found at the greatest depth within the film. Thus, referring to figure 11*c*, the arrows indicate the relative distances moved by Al^{3+} ions and tungsten species. Therefore tungsten species migrate at about 25% of the rate of Al^{3+} ions. Similarly, molybdenum species migrate at about 50% of the rate of Al^{3+} ions. Since the distribution of tungsten in the film does not change significantly on changing the anodizing conditions, by implication the mobility of tungsten species with respect to Al^{3+} ions is relatively invariant, paralleling the similar invariance of Al^{3+} and O^{2-}/OH^{-} migration. Thus, it is highly probable that the migration of tungsten and molybdenum species is determined by the cooperative transport process that controls Al^{3+} and O^{2-}/OH^{-} migration.

PHILOSOPHICAL TRANSACTIONS OF THE ROYAL SOCIETY A MATHEMATICAL, PHYSICAL & ENGINEERING SCIENCES

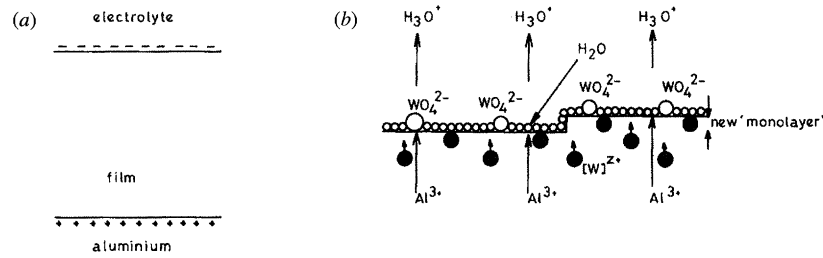

Figure 12. Incorporation of electrolyte species. (*a*) Capacitor model of the film, in which adsorbed anions form the double layer charge density at the film surface. (*b*) Schematic diagram illustrating the incorporation of tungsten species into a film. Al^{3+} ions react with adsorbed tungstate ions resulting in the incorporation of the mobile species $[W]^{Z+}$.

(*c*) *Incorporation of molybdenum and tungsten*

Unlike many features of anodic films, the physical and chemical structure of the film–electrolyte interface during anodizing is poorly characterized. Here, complex interacting processes occur simultaneously, resulting in the transport of ions and molecules, the formation of new film material, the maintenance of the double layer charge density and the establishment of a local environment that is markedly different from the bulk electrolyte chemistry. Further, the incorporation of molybdenum and tungsten may in principle depend upon a large number of kinetic and thermodynamic factors. The electrolyte anions must contribute substantially to the double layer charge density which is essential to film formation. These may be adsorbed on the film, or may be contained in the adjacent electrolyte in the diffuse layer. However, if the solution is concentrated, the diffuse layer may be disregarded since it only provides a small amount of excess charge.

A simple capacitor model of the film is considered to explain the incorporation of tungsten species as illustrated in figure 12*a*. A similar approach can be used for the incorporation of molybdenum species. The film supports the electric field generated by the charge densities on the metal surface and in the electrolyte. The latter charge density is assumed to be due to adsorbed anions. At the film–electrolyte interface, Al^{3+} ions react mainly with water molecules to form new film material. As each 'monolayer' of film material is added at the film–electrolyte interface, the adsorbed tungstate ions are transformed on incorporation into the film to an outwardly mobile electrolyte species, as shown in figure 12*b*. Each 'monolayer' of film, consisting mainly of Al_2O_3, incorporates all of the adsorbed anions. Hence, the film composition can be calculated from the density of adsorbed anions, the 'monolayer' thickness and the fraction of the film thickness formed at the film–electrolyte interface. The incorporated anions are replaced by anions from the electrolyte that are adsorbed on the newly formed surface.

To test this idea, let the adsorbed tungstate anions contribute the full double layer charge density, σ, since the concentration of hydroxide ions is low in the bulk electrolyte. The double layer charge density can be calculated from,

$$\sigma = \epsilon_r \epsilon_0 E, \tag{4.1}$$

in which ϵ_r is the dielectric constant of the film, ϵ_0 is the permittivity of free space, and E is the electric field strength across the film. Using available data for anodizing at 50 A m^{-2} at 293 K (Harkness & Young 1966), $\sigma \approx 7.2 \times 10^{-2}$ C m^{-2},

PHILOSOPHICAL TRANSACTIONS OF THE ROYAL SOCIETY A MATHEMATICAL, PHYSICAL & ENGINEERING SCIENCES

that is equivalent to 2.25×10^{17} tungsten atoms m^{-2} which are present in WO_4^{2-} ions. The adsorbed tungsten is assumed to be incorporated completely by each new 'monolayer' of film material formed at the film–electrolyte interface. A rough estimate of the interatomic separation of oxygen in the film is used as the 'monolayer' thickness, namely,

$$\left(\frac{M}{3\rho N_A}\right)^{1/3}, \tag{4.2}$$

in which ρ is the film density ($3100\ kg\ m^{-3}$), M is the molecular mass of the film and N_A is Avogadro's number. This gives a 'monolayer' thickness of about 0.26 nm. For film formation at 100% efficiency, an average atomic ratio of W/Al in the film of about 9×10^{-3} is predicted. This agrees reasonably well with the measured ratio of about 7×10^{-3}. Less tungsten is expected in films formed in more dilute electrolytes since the thickness of the double layer increases and a greater proportion of the tungstate ions are contained in the diffuse region. This qualitatively explains the 35% decrease in concentration found between electrolyte concentrations of 10^{-5}–10^{-1} M. The 15% increase in the tungsten concentration in films formed at current densities between 20 and 1000 A m^{-2} corresponds well with a predicted increase of about 14% in the double layer charge density. However, the effect of temperature shows a poor correlation. The measured increase of 50% in tungsten concentration in films formed between 273–323 K compares with a predicted reduction of 9% in the double layer charge density using the electric field strengths of Harkness & Young. This possibly reflects additional effects of temperature on factors such as adsorption, chemical equilibria, ionic diffusion coefficients in the electrolyte, and possibly the structure of the film surface, which affect the concentration of anions at the film surface. However, interestingly other investigators have indicated an opposite trend in electric field strengths to that of Harkness & Young, i.e. an increase of about 10% between 293–333 K (Takahashi & Nagayama 1978). This trend is consistent with an increase in the concentration of tungsten with temperature, as found experimentally at lower temperatures, although the temperature range of their measurements does not extend down to 273 K to allow a complete comparison. Such an increase in field strength with temperature might occur if the film is more resistive at higher temperatures due to the development of microcrystallinity.

The main film-forming reaction at the film–electrolyte interface, by which H_3O^+ ions are also generated at the film surface, is:

$$2Al^{3+}_{film} + 9H_2O \rightarrow Al_2O_3 + 6H_3O^+. \tag{4.3}$$

Incorporation of tungsten is possible by reaction of the adsorbed tungstate ions at the film surface either with Al^{3+} ions, according to the overall reaction:

$$2Al^{3+}_{film} + [WO_4^{2-}]_{ads} + 6H_2O \rightarrow WO_3 + Al_2O_3 + 4H_3O^+, \tag{4.4}$$

or with H_3O^+ ions, according to the reaction (Pourbaix 1974):

$$[WO_4^{2-}]_{ads} + 2H_3O^+ \rightarrow WO_3 + 3H_2O. \tag{4.5}$$

Tungsten is introduced into the film as WO_3 by both of the above reactions, and may be subsequently mobile as a WO_2^{2+}, WO^{4+} or W^{6+} cation. The lower mobility of tungsten species compared with Al^{3+} ions possibly indicates the presence of WO_2^{2+} ions, which have both a lower charge and larger size than Al^{3+} ions. The

introduction of WO_3 is consistent with the film composition deduced from the atomic ratios of aluminium, oxygen and tungsten in the film, determined by RBS. The possibility that the measured excess oxygen, i.e. above that needed for Al_2O_3, is due to OH^- ions or water is discounted, since the H/Al atomic ratio in barrier-films, measured using a nuclear reaction, is a factor of *ca.* 5 too low (Lanford *et al.* 1980). By implication, since the amount of tungsten species in the film is low, the water molecules in the electrolyte are the main source of oxygen for film formation. The concentration of electrolyte species in the film indicates that about 2 at/o of the oxygen atoms are derived from tungstate ions. A fraction of these oxygen atoms introduced with the tungsten may remain associated with the tungsten during film formation, as WO_2^{2+} for instance.

MoO_3 and WO_3 are glass formers, and may be integrated into the alumina structure. Structural studies of anodic alumina have indicated the presence of AlO_4, AlO_5 and AlO_6 polyhedra (Oka *et al.* 1979). 'Defects' may be created due to the 6+ state of the molybdenum and tungsten. Further, the alumina structure is relatively open, since the density is about 15% lower than that of crystalline alumina. Thus, alternatively the electrolyte species may be accommodated in voids, leaving the Al^{3+} ionic density in the film relatively unchanged. The two possibilities are not distinguishable from the step in the aluminium peak of figure 3, both of which would produce similar effects. Incorporated electrolyte species are able to stabilize the structure against crystallization during exposure of the film in the electron beam of the TEM (Shimizu *et al.* 1981). This allows distributions of electrolyte species to be inferred from preferential crystallization of the relatively pure regions.

(*d*) *Interfacial chemistry*

During anodizing, the pH at the film surface is lowered by generation of H_3O^+ ions by (4.3). The tendency towards acidification can be assessed for a neutral or slightly alkaline solution from the equation,

$$J = -(FD/\delta)(C^{\mathrm{i}}_{H_3O^+} - C^{\mathrm{b}}_{H_3O^+}), \tag{4.6}$$

in which $C^{\mathrm{i}}_{H_3O^+}$ and $C^{\mathrm{b}}_{H_3O^+}$ are the concentration of H_3O^+ ions at the film surface and in the bulk electrolyte, D is the diffusion coefficient of H_3O^+ ions, δ is the thickness of the diffusion layer, F is the faraday and J is the ionic current density (Leach & Pearson 1984). For $J = 50\ \mathrm{A\ m^{-2}}$, $D = 10^{-8}\ \mathrm{m^2\ s^{-1}}$, $\delta = 5 \times 10^{-5}\ \mathrm{m}$ and $C^{\mathrm{b}}_{H_3O^+} = 10^{-9}$ M (roughly the concentration in 10^{-1} M tungstate electrolyte), the interfacial pH is 2.6. The pH decreases by 1 unit per ten-fold increase in ionic current density.

In practice, the decline in pH is limited by chemical equilibria with electrolyte anions; for the anions of present interest these are of the type:

$$WO_4^{2-} + 2H_3O^+ \rightleftharpoons WO_3 + 3H_2O. \tag{4.7}$$

The tungstate ions react with H_3O^+ ions to form tungsten oxide, which is probably hydrated. For tungstate ion concentrations of 10^{-4}–10^{-1} M, the equilibrium pH for the reaction at 25 °C ranges from 5.0 to 6.5 (Pourbaix 1974). Thus, as the film surface is approached, the concentration of tungstate ions decreases below the concentration in the bulk electrolyte and tungsten oxide is formed and dispersed from the interfacial electrolyte. The reaction prevents the pH falling to

PHILOSOPHICAL TRANSACTIONS OF THE ROYAL SOCIETY A MATHEMATICAL, PHYSICAL & ENGINEERING SCIENCES

a strongly acidic value. At the film surface, the concentration of tungstate ions rises to establish the double layer charge.

The solubility of alumina is a minimum at pH 5 and increases as the pH moves away from this value (Pourbaix 1974). Since the reaction of WO_4^{2-} and H_3O^+ ions maintains the interfacial pH near to the solubility minimum and in a range in which direct ejection of Al^{3+} ions to solution is negligible, the films are formed at high efficiency. The efficiency of film formation depends upon the degree of competition from direct ejection of Al^{3+} ions into the solution at the film surface, which is promoted by a lower interfacial pH. However, anodizing at high efficiency is assisted by a high current density. Thus, the film formation rate increases more rapidly than the rate of direct ejection of Al^{3+} ions with increase in electric field, despite the tendency towards a lower interfacial pH from a faster rate of H_3O^+ ion generation.

At pH $\leqslant$ 11, the concentration of OH^- ions in the bulk electrolyte is too low to prevent the interfacial pH declining to a slightly acidic value. The OH^- ions are depleted in the interfacial electrolyte by reaction with the relatively abundant H_3O^+ ions. The residual H_3O^+ ions react with tungstate ions as described previously. Therefore, increasing the pH, of the bulk electrolyte to 11 has only a minor effect on the interfacial pH. Tungstate remains the main double layer anion, and hence the film compositions are unaffected. Above pH 11, the supply of OH^- ions is sufficient to create an alkaline interfacial pH. The interfacial pH changes sharply from acidic to alkaline for a relatively small change in the pH of the bulk electrolyte (Leach & Pearson 1984). This explains the rapid decline in the efficiency of film formation above a bulk electrolyte pH of 11.

As the efficiency of film formation decreases in the increasingly alkaline interfacial environment, less film material forms at the film–electrolyte interface. A longer time is needed to form each fresh 'monolayer', during which the mobile tungsten species from underlying layers can move to the surface. Since WO_3 is unstable at pH $>$ 7, leaching of tungsten may also occur. Thus, the amount of tungsten in films falls rapidly above pH 11. Owing to its mobility in the film, no tungsten should be incorporated when the efficiency of film formation is less than 70%; any tungsten oxide formed should remain at the film surface and dissolve in the electrolyte as WO_4^{2-}. The small amount of tungsten found in the film formed in the electrolyte of pH 12.1, when the efficiency was about 50% is probably due to residual tungstate ions from the electrolyte trapped in a finely porous and/or hydrated surface.

The enhanced concentration of tungsten on specimens anodized at less than 10 A m^{-2} is mainly associated with oxide precipitation, due to reaction (4.5), at the film surface, that in other circumstances is dispersed in the bulk electrolyte as oxide particles which subsequently dissolve. The precipitated oxide at the film surface is gel-like and is hydrated, and is to be considered in detail in a subsequent paper.

The precipitation of oxide is possibly the origin of the very thin 'layers' containing sub-monolayer concentrations of molybdenum or tungsten at the film surfaces of specimens anodized at higher current density, found previously by RBS (Skeldon *et al.* 1989). Thus, if the oxide molecules are not efficiently dispersed in the bulk electrolyte, colloidal particles may nucleate and aggregate as islands, or possibly form gel-like layers, at the film surface. Their presence may explain the scatter observed in film compositions in the various figures presented.

There is no evidence from the voltage-time curves that they affect the anodizing behaviour, suggesting that they are incomplete, porous or permeable structures. On the other hand, if the 'layers' function as semi-permeable membranes, they might afford the film some protection against dissolution in acidic interfacial conditions. Alternatively the sub-monolayer concentrations may be merely residual contamination from the electrolyte.

Oxide may also precipitate and be trapped at flaws in films forming at high efficiency. These are regions where film development is impaired by secondary electrochemical reactions occurring at fine impurity segregates on the original metal surface (Shimizu *et al.* 1984). In effect, channels are created in which oxide may precipitate in acidic conditions, such as would be promoted by oxygen evolution. The flaws 'heal' as the impurity is undermined by film formation. The oxide would then be incorporated into the film as a tungsten-enriched pocket of material. The pockets could occur in the inner regions of film not accessible to tungsten incorporated in the usual manner. The density of flaws in films formed on superpure aluminium is extremely low and would have negligible effect on the film composition even if internal oxide is precipitated. Further TEM studies are needed, possibly using aluminium alloys on which films form with a high flaw density, to detect the presence of oxide pockets, or otherwise.

In the vicinity of flaws, enhanced Joule heating can occur because of the high current density at flaw sites, and on occasions, crystalline film material is observed. The localized heating may increase the concentration of tungsten in film material near flaws, following the trend of increased incorporation found for higher electrolyte temperatures. Joule heating is slight during normal anodizing, but significant temperature rises are found at very high current density (Applewhite *et al.* 1969). Thus, rises of 15–30 K can be produced at 1000 A m^{-2}, which may have a small effect on the film composition at this current density.

(*e*) *Films formed in electrolytes containing both molybdate and tungstate ions*

The films formed in mixed electrolytes reveal preferential incorporation of one electrolyte species. Which species is preferred depends particularly upon the current density. Thus, during anodizing in electrolytes containing equal concentrations of molybdate and tungstate anions in the bulk electrolyte, tungsten species are preferentially incorporated into the film at 50 A m^{-2}, and molybdenum species at 200 A m^{-2}. However, if the concentrations of molybdate and tungstate ions in the bulk electrolyte differ by a factor of ten or more, the film composition is determined by the dominant anion. Notably, anodizing in electrolytes containing both anions does not increase the total concentration of electrolyte species in the film, compared with anodizing in the individual electrolytes. Therefore, whenever both electrolyte species are incorporated into a film, their concentrations are lower than in films formed in individual electrolytes. The similarity of total levels of incorporation shows that the total concentration of adsorbed anions at the film surface is about the same for anodizing in electrolytes containing molybdate, tungstate or a mixture of molybdate and tungstate ions.

Preferential incorporation is dependent upon the concentrations of molybdate and tungstate anions in the interfacial electrolyte, upon which the adsorption of a particular anion depends. The differences between the interfacial and bulk electrolyte compositions primarily occur because of reactions of the anions with the H_3O^+ ion flux, generated by film formation. Depletion of anions due to loss

PHILOSOPHICAL TRANSACTIONS OF THE ROYAL SOCIETY A MATHEMATICAL, PHYSICAL & ENGINEERING SCIENCES

of anions to the film is comparatively negligible because of the low concentrations of incorporated electrolyte species. For similar concentrations of molybdate and tungstate ions in solution, the formation of MoO_3 takes place at a much lower pH than the formation of WO_3 (Pourbaix 1974). Thus, tungstate anions are depleted in the interfacial electrolyte rather than molybdate ions. The possibility of the formation of polymolybdate ions is not considered because of the uncertainty in their occurrence under the particular interfacial conditions of anodizing. The depletion of tungstate ions near the film surface is greater at higher current density, because of the higher rate of H_3O^+ ion generation, and results in a steeper concentration gradient of tungstate ions in the interfacial electrolyte.

The relative concentrations of molybdate and tungstate ions in the interfacial region depend upon the kinetics of anion consumption, as determined by the current density, and supply from the electrolyte, determined particularly by the concentration and temperature of the electrolyte. The present results reveal that at a current density of 200 A m^{-2}, the film contains significantly more molybdenum species than tungsten species, which indicates that under these conditions the rate of supply from the bulk electrolyte is insufficient to prevent significant depletion of tungstate ions at the film surface. Therefore, more molybdate ions than tungstate ions are adsorbed, and hence the films contain mainly incorporated molybdenum species. At a lower current density of 50 A m^{-2}, the depletion of tungstate ions is reduced. Although now the concentration of tungstate ions in the interfacial electrolyte is higher, it is still less than that of molybdate ions, since tungstate ions are consumed preferentially by reaction with H_3O^+ ions. However, the film contains mainly tungsten species, indicating that tungstate ions are preferentially adsorbed, presumably because the kinetics of adsorption are more favourable than for molybdate ions. However, if the concentration of tungstate ions in the bulk electrolyte is significantly reduced with respect to the concentration of molybdate ions, the supply of tungstate ions to the film surface decreases, less tungstate ions are adsorbed on the film surface, and the resultant films contain mainly molybdenum.

The distributions and hence, migration rates, of the electrolyte species in films formed in the mixed electrolytes are the same as those in films formed in the relevant individual electrolytes, i.e. molybdenum and tungsten species are found in the outer 0.2 and 0.3 of the film thickness, respectively. However, since the total concentration of electrolyte species within the films does not exceed that found for the individual electrolytes, the point concentrations of molybdenum and tungsten are less than their usual values. For example, the point concentrations of molybdenum and tungsten in films formed at 50 A m^{-2} in individual 10^{-1} M molybdate and tungstate electrolytes are about 3.3×10^{-2} and 2.5×10^{-2}, whereas in a film formed at 50 A m^{-2} in an electrolyte containing 5×10^{-2} M of both molybdate and tungstate ions, when tungsten species are preferentially incorporated, they are about 0.6×10^{-2} and 2.1×10^{-2} respectively. At these relatively low concentrations of electrolyte species, the molybdenum and tungsten species migrate at their usual rates. Possibly small numbers of the species do suffer a change in migration rate due to mutual interactions, but other analysis techniques would be required to detect these.

Interestingly, the stability of the films against crystallization in the TEM is rather sensitive to either the type of electrolyte species or the concentration of the electrolyte species in the film. The film investigated by TEM, which was formed

at 50 A m^{-2} in an electrolyte containing molybdate and tungstate ions in concentrations of 5×10^{-2} M crystallized sequentially to reveal three regions. The first region extends from a depth of about 0.3 of the film thickness to the metal–film interface, and is a region of relatively pure anodic alumina that is the most unstable in the electron beam. The second region, between depths of 0.2–0.3 of the film thickness, contains tungsten species only, with a point concentration of about 2.1×10^{-2}. The final outer 0.2 of the film thickness contains both molybdenum and tungsten species with a combined point concentration of about 2.7×10^{-2}. Thus, the sequence of crystallization follows the increase in concentration of electrolyte species in the film. Possibly also, molybdenum species, present only in the outermost region, have a greater influence on film stability than tungsten species, hence providing additional film stability than simply due to the higher total concentration of electrolyte species.

5. Conclusions

1. Electrolyte species are incorporated into anodic films formed in molybdate and tungstate electrolytes by the transformation of electrolyte anions to cationic species in the film. The mechanism involves reaction of Al^{3+} ions, that have migrated across the film, with anions adsorbed on the film surface, resulting in the introduction of MoO_3 or WO_3 into the film. Subsequently, species of the type XO_2^{2+}, XO^{4+} or X^{6+} are created resulting in the outward migration of both molybdenum and tungsten.

2. Ionic migration in the film is controlled by a cooperative transport mechanism involving Al^{3+} and O^{2-}/OH^- ions and the cationic electrolyte species. This fixes the relative migration rates of the ions in the film, relatively independently of the anodizing conditions, although a particular electrolyte species has a unique migration rate. Molybdenum species migrate more rapidly than tungsten species, so they are contained in a narrower band of film material.

3. The incorporation of electrolyte species may be understood in terms of a simple capacitor model of the film in which adsorbed electrolyte anions form the double layer charge density. At least for outwardly mobile electrolyte species, the incorporation is dependent upon formation of film material at the film–electrolyte interface. In the films formed at high efficiency, the adsorbed electrolyte anions are transformed and incorporated during growth of new film material at the film–electrolyte interface. The amount of electrolyte species in the film formed under different anodizing conditions can be related to the double layer charge density, which is due mainly to adsorbed anions, although temperature variations introduce additional effects that need further investigation. During formation at low efficiency and in the absence of film formation at the film–electrolyte interface, electrolyte anions are not incorporated into the film. Such films may, however, contain precipitated oxide or residual electrolyte contamination in porous surface layers.

4. Molybdate and tungstate ions are similarly adsorbed on the film surface and incorporated into the film and hence, the concentrations of the respective electrolyte species in the films formed in the individual electrolytes are similar. Further, for films formed in electrolytes containing both molybdate and tungstate ions, the total concentration of incorporated electrolyte species cannot exceed

PHILOSOPHICAL TRANSACTIONS OF THE ROYAL SOCIETY A MATHEMATICAL, PHYSICAL & ENGINEERING SCIENCES

that in films formed in the individual electrolyte, because the double layer charge density is not significantly changed.

5. The relative proportions of molybdenum and tungsten species incorporated into the film depends upon the composition of the electrolyte adjacent to the film surface. This is modified from the bulk electrolyte composition due to reaction of H_3O^+ ions with molybdate and tungstate ions. In particular the reaction occurs preferentially with the tungstate ions which tends to deplete the interfacial electrolyte of these ions. The extent of depletion depends upon the current density and the concentration of tungstate ions in the bulk electrolyte. However, the kinetics of adsorption of molybdate and tungstate ions are also important. Thus, depending upon the anodizing conditions either molybdenum species or tungsten species are preferentially incorporated into the film.

6. In all cases, the amounts of electrolyte species in the film are small corresponding to average atomic ratios of either molybdenum or tungsten to aluminium of about 7×10^{-3}. Locally the concentration of molybdenum is about 30% higher than that of tungsten because it is contained within a narrower band of film material as a result of its higher mobility. In films formed in mixed electrolytes the concentrations of electrolyte species in their respective layers are lower than in films formed in the individual electrolytes. At these relatively low concentrations the two species are able to migrate in the film with their usual mobilities.

7. The tendency toward acidification of the interfacial electrolyte and the reaction of H_3O^+ ions with the anions are important in determining the efficiency of film formation. The efficiency is high if the interfacial pH is in the near neutral to slightly acidic range in which alumina is relatively stable.

The authors thank the Science and Engineering Research Council for the award of a Research Assistantship to P.S. and the Royal Society for a Guest Visiting Fellowship taken up by K.S.

Appendix A. Analysis of anodic films by RBS

The principles of RBS are well-established (Chu *et al.* 1978). However, a brief description is given here of the approach used to analyse thin anodic films. The yield, Y_i, of alpha particles elastically scattered from element i, in a film of thickness t, is given approximately by

$$Y_i = C_0 \int_0^t N_i(x)\sigma_i(x)\,\mathrm{d}x, \tag{A 1}$$

in which $N_i(x)$ and $\sigma_i(x)$ are the atomic density and cross section respectively for elastic scattering for element i at depth x, and C_0 is a constant that depends upon the beam current, analysis time and parameters of the detection system. Straggling, causing the beam energy to be increasingly spread with penetration of the film, can be neglected for thin films without significantly affecting the analysis. The mean energy of alpha particles at depth x, $E(x)$, is given by

$$E(x) = E_0 - Sx, \tag{A 2}$$

in which E_0 is the energy of the incident beam and S is the stopping power of the film. The stopping power is approximately constant for thin films. The

distributions of molybdenum and tungsten in the respective films are given by

$$\left.\begin{aligned} N_i(x) &= N_i, \quad 0 \leqslant x \leqslant x_i, \\ N_i(x) &= 0, \quad x_i \leqslant x \leqslant t. \end{aligned}\right\} \tag{A 3}$$

From equations (A 1), (A 2) and (A 3):

$$Y_i = \frac{C_0 N_i}{S} \int_{E_0 - S x_i}^{E_0} \sigma_i(E)\, \mathrm{d}E. \tag{A 4}$$

For the elements of interest, the Rutherford expressions for the elastic scattering cross-sections can be used (MacDonald *et al.* 1983). Thus $\sigma_i(E) = K_i/E^2$ in which K_i can be calculated. Substitution of this relation into equation (A 4), followed by integration, gives

$$Y_i = \frac{C_0 N_i K_i S x_i}{E_0(E_0 - S x_i)}. \tag{A 5}$$

The average atomic ratio of elements i and j is therefore

$$\frac{N_i x_i}{N_j x_j} = \frac{Y_i K_j E_0 (E_0 - S x_i)}{Y_j K_i E_0 (E_0 - S x_j)}. \tag{A 6}$$

For i and j being tungsten and aluminium respectively, this atomic ratio is referred to in the paper as the average concentration of tungsten in the film. For aluminium, N_{Al} is approximately constant across the film thickness.

The thickness of the region of film containing element i, x_i can be determined from the width, ΔE_i, of the yield for element i given by

$$\Delta E_i = [S_i] x_i, \tag{A 7}$$

in which $[S_i]$ is the energy loss factor for element i. The method, however, is limited by the energy resolution of the surface barrier detector. This was greater than 20 keV, depending upon the particular detector used. For normal beam incidence on the film, the depth resolution was typically more than 50 nm. In general, the distributions of molybdenum and tungsten were not adequately resolved in films formed to 200–250 V. Measurements of distributions were therefore only made for films formed to higher voltages, i.e. for substantially thicker films, or for films that were angled to increase the film thickness in the beam direction and improve the effective depth resolution. The distributions were derived from $\Delta E_i/\Delta E_{\mathrm{Al}}$, using experimental values of stopping powers to calculate the energy loss factors (Skeldon *et al.* 1983). Thus, the fractions of the film thickness containing element i, x_i/t, were obtained.

Compositions were also determined for some films from the yields per channel due to elastic scattering from tungsten nuclei, H_{W}, and aluminium nuclei, H_{Al}, in the outer region of film containing the electrolyte species. The films were angled to the beam to ensure that the yields were unaffected by the detector resolution. The atomic ratio of tungsten to aluminium in the outer region of film is given by

$$\frac{N_{\mathrm{W}}}{N_{\mathrm{Al}}} = \frac{H_{\mathrm{W}} K_{\mathrm{Al}} [S_{\mathrm{W}}]}{H_{\mathrm{Al}} K_{\mathrm{W}} [S_{\mathrm{Al}}]}. \tag{A 8}$$

This atomic ratio is referred to in the paper as the point concentration of tungsten

PHILOSOPHICAL TRANSACTIONS OF THE ROYAL SOCIETY A MATHEMATICAL, PHYSICAL & ENGINEERING SCIENCES

in the film, in order to distinguish it clearly from the average concentration of tungsten referred to previously. The point concentration of tungsten is converted to the average concentration by multiplying by the fraction of the film thickness in which the tungsten is contained.

References

Amsel, G. & Samuel, D. 1962 The mechanisms of anodic oxidation. *J. Phys. Chem. Solids* **23**, 1707–1718.

Applewhite, F. R., Leach, J. S. L. & Neufeld, P. 1969 The temperature rise during anodizing of aluminium. *Corros. Sci.* **9**, 305–308.

Brown, F. & Mackintosh, W. D. 1973 The use of Rutherford backscattering to study the behaviour of ion implanted atoms during anodic oxidation of aluminium; Ar, Kr, Xe, K, Rb, Cs, Cl, Br and I. *J. Electrochem. Soc.* **120**, 1096–1102.

Chu, W. K., Mayer, J. W. & Nicolet, M.-A. 1978 *Backscattering spectrometry*. Academic Press.

Chung, S., Robinson, J., Thompson, G. E., Wood, G. C. & Isaacs, H. S. 1991 An X-ray absorption study of barrier-type anodic films formed on aluminium in chromate electrolytes. *Phil. Mag.* B **63**, 557–571.

Davies, J. A., Domeij, B., Pringle, J. P. S. & Brown, F. 1965 The migration of metal and oxygen during anodic film formation. *J. Electrochem. Soc.* **112**, 675–680.

Dell'Oca, C. J. & Young, L. 1970 High-field ionic conduction in tantalum anodic oxide films with incorporated phosphate. *J. Electrochem. Soc.* **117**, 1548–1551.

Dignam, M. J. 1972 *Oxide and oxide films* (ed. J. W. Diggle), vol. 1, pp. 91–256. New York: Marcel Dekker.

Dignam, M. J., Goad, D. & Sole, M. 1965 Determination of the field dependence of the Tafel slope for the steady state anodic oxidation of aluminium. *Can. J. Chem.* **43**, 800–808.

Di Quarto, F., Piazza, S., Splendore, A. & Sunseri, C. 1992 More insights on the photocurrent behaviour of the aluminium/aluminium oxide/electrolyte junction. In *Oxide films on metals and alloys* (ed. B. R. MacDougall, R. S. Alwitt & T. A. Ramanarayanan), pp. 311–325. New Jersey: The Electrochemical Society.

Fromhold, A. T. 1980 Nonsimultaneous place exchange: a microscopic high field transport mechanism in solids. *J. Electrochem. Soc.* **127**, 411–425.

Furneaux, R. C., Thompson, G. E. & Wood, G. C. 1978 The application of ultramicrotomy to the electronoptical study of surface films on aluminium. *Corros. Sci.* **18**, 853–881.

Harkness, A. C. & Young, L. 1966 High resistance anodic oxide films on aluminium. *Can. J. Chem.* **44**, 2409–2413.

Konno, H., Kobayashi, S., Fujimoto, K., Takahashi, H. & Nagayama, M. 1980 Composition of barrier type oxide films anodically formed on aluminium in a neutral borate solution. *Electrochim. Acta* **25**, 1667–1672.

Lanford, W. A., Alwitt, R. S. & Dyer, C. K. 1980 Hydrogen profiles of anodic aluminium oxide films. *J. Electrochem. Soc.* **127**, 405–411.

Leach, J. S. L. & Pearson, B. R. 1984 The conditions for incorporation of electrolyte ions into anodic oxides. *Electrochim. Acta* **29**, 1263–1270.

MacDonald, J. R., Davies, J. A., Jackman, T. E. & Feldman, L. C. 1983 How well does the backscattering from low-Z nuclei obey the Rutherford formula? *J. appl. Phys.* **54**, 1800–1803.

Montero, I., Albella, J. M. & Martinez-Duart, J. M. 1985 Influence of electrolyte concentration on the anodization and breakdown of Ta_2O_5 films. *J. Electrochem. Soc.* **132**, 814–818.

Mott, N. F. 1987 On the oxidation of silicon. *Phil. Mag.* B **55**, 117–129.

Oka, Y., Takahashi, T., Okada, K. & Iwai, S. 1979 Structural analysis of anodic alumina films. *J. non-cryst. Sol.* **30**, 349–357.

Perriere, J., Pelloie, B. & Siejka, J. 1987 Ionic movement during oxide growth by plasma anodization. *Phil. Mag.* B **55**, 271–289.

PHILOSOPHICAL TRANSACTIONS OF THE ROYAL SOCIETY A MATHEMATICAL, PHYSICAL & ENGINEERING SCIENCES

Pourbaix, M. 1974 *Atlas of electrochemical equilibria in aqueous solutions.* Houston, Texas: National Association of Corrosion Engineers.

Pringle, J. P. S. 1973 The migration of oxygen during the anodic oxidation of tantalum. *J. Electrochem. Soc.* **120**, 1391–1400.

Pringle, J. P. S. 1980 The anodic oxidation of superimposed metallic layers: theory. *Electrochim. Acta* **25**, 1423–1437.

Shimizu, K., Thompson, G. E. & Wood, G. C. 1981 Direct observation of the duplex nature of anodic barrier films on aluminium. *Thin Solid Films* **81**, 39–44.

Shimizu, K., Skeldon, P., Thompson, G. E. & Wood, G. C. 1982 Preparation of self-supporting anodic barrier films on aluminium for backscattering analysis. *Surf. Interface Analysis* **4**, 208–211.

Shimizu, K., Kobayashi, K., Thompson, G. E. & Wood, G. C. 1984 Flaws in anodic barrier films on aluminium. *J. Met. Finish. Soc. Jpn.* **35**, 374–382.

Shimizu, K., Kobayashi, K., Thompson, G. E. & Wood, G. C. 1990 The unusual distribution of chromium in barrier-type anodic oxide films on aluminium. *J. Surf. Finish. Soc. Jpn* **40**, 1441–1442.

Shimizu, K., Kobayashi, K., Thompson, G. E. & Wood, G. C. 1991 A novel marker for the determination of transport numbers during anodic barrier-type oxide growth on aluminium. *Phil. Mag.* B **64**, 345–353.

Skeldon, P., Shimizu, K., Thompson, G. E. & Wood, G. C. 1983 Barrier-type anodic films on aluminium in aqueous borate solutions. 1. Film density and stopping power of anodic alumina films for alpha particles. *Surf. Interface Analysis* **5**, 247–251.

Skeldon, P., Shimizu, K., Thompson, G. E. & Wood, G. C. 1985 Fundamental studies elucidating anodic barrier-type film growth on aluminium. *Thin Solid Films* **123**, 127–133.

Skeldon, P., Skeldon, M., Thompson, G. E. & Wood, G. C. 1989 Incorporation of tungsten and molybdenum species into anodic alumina films. *Phil. Mag.* B **60**, 513–521.

Skeldon, P., Shimizu, K., Thompson, G. E. & Wood, G. C. 1990 Direct observations of anodic film growth on superimposed aluminium and tantalum metallic layers. *Phil. Mag.* B **61**, 927–938.

Skeldon, M., Skeldon, P., Thompson, G. E., Wood, G. C. & Shimizu, K. 1993 Formation of barrier anodic films on aluminium in antimonate electrolyte. *Phil. Mag.* B **68** 787–803.

Takahashi, H. & Nagayama, M. 1978 Electrochemical behaviour and structure of anodic oxide films formed on aluminium in neutral borate solution. *Electrochim. Acta* **23**, 279–286.

Thompson, G. E., Xu, Y., Skeldon, P., Shimizu, K., Han, S. H. & Wood, G. C. 1987 Anodic oxidation of aluminium. *Phil. Mag.* B **55**, 651–667.

Young, L. 1960 Steady-state kinetics of formation of anodic oxide films on tantalum in sulphuric acid. *Proc. R. Soc. Lond.* A **258**, 496–515.

Young, L. & Smith, D. J. 1979 Models for ionic conduction in anodic oxide films. *J. Electrochem. Soc.* **126**, 765–768.

Received 25 June 1993; accepted 26 August 1993

PHILOSOPHICAL TRANSACTIONS OF THE ROYAL SOCIETY A MATHEMATICAL, PHYSICAL & ENGINEERING SCIENCES

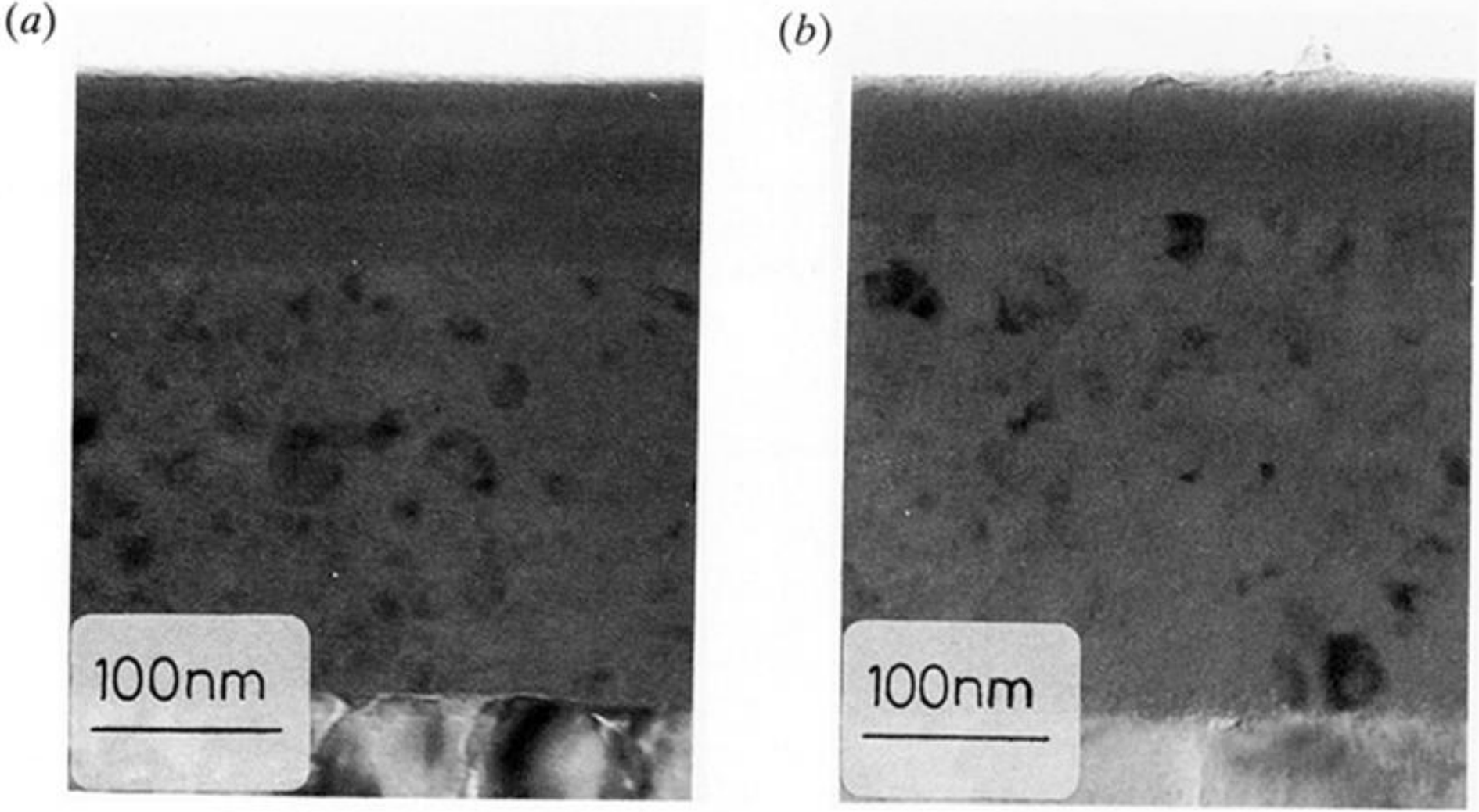

'igure 9. Transmission electron micrographs of an ultramicrotomed section of a film formed at 0 A m^{-2} to 285 V in an electrolyte containing 5×10^{-2} M of both molybdate and tungstate ions t 293 K and crystallized in the electron beam of the TEM. (*a*) Initial location of the boundary etween crystallized and uncrystallized film material. (*b*) Subsequent location of the boundary n further exposure to the electron beam.

PHILOSOPHICAL TRANSACTIONS OF THE ROYAL SOCIETY A MATHEMATICAL, PHYSICAL & ENGINEERING SCIENCES